Magn Reson Med Sci 2023; 22; 353–360
doi:10.2463/mrms.mp.2022-0020 Published Online: July 9, 2022

MAJOR PAPER

Commercially Available Deep-learning-reconstruction of MR Imaging of the Knee at 1.5T Has Higher Image Quality Than Conventionally-reconstructed Imaging at 3T: A Normal Volunteer Study

Hiroyuki Akai[1,2], Koichiro Yasaka[2,3], Haruto Sugawara[1], Taku Tajima[2,4], Masaaki Akahane[2], Naoki Yoshioka[2], Kuni Ohtomo[5], Osamu Abe[3], and Shigeru Kiryu[2*]

Purpose: This study aimed to evaluate whether the image quality of 1.5T magnetic resonance imaging (MRI) of the knee is equal to or higher than that of 3T MRI by applying deep learning reconstruction (DLR).

Methods: Proton density-weighted images of the right knee of 27 healthy volunteers were obtained by 3T and 1.5T MRI scanners using similar imaging parameters (21 for high resolution image and 6 for normal resolution image). Commercially available DLR was applied to the 1.5T images to obtain 1.5T/DLR images. The 3T and 1.5T/DLR images were compared subjectively for visibility of structures, image noise, artifacts, and overall diagnostic acceptability and objectively. One-way ANOVA and Friedman tests were used for the statistical analyses.

Results: For the high resolution images, all of the anatomical structures, except for bone, were depicted significantly better on the 1.5T/DLR compared with 3T images. Image noise scored statistically lower and overall diagnostic acceptability scored higher on the 1.5T/DLR images. The contrast between lateral meniscus and articular cartilage of the 1.5T/DLR images was significantly higher (5.89 ± 1.30 *vs.* 4.34 ± 0.87, $P < 0.001$), and also the contrast between medial meniscus and articular cartilage of the 1.5T/DLR images was significantly higher (5.12 ± 0.93 *vs.* 3.87 ± 0.56, $P < 0.001$). Similar image quality improvement by DLR was observed for the normal resolution images.

Conclusion: The 1.5T/DLR images can achieve less noise, more precise visualization of the meniscus and ligaments, and higher overall image quality compared with the 3T images acquired using a similar protocol.

Keywords: *artificial intelligence, deep learning, magnetic resonance imaging, knee*

Introduction

Although 1.5T MRI has been the standard modality for knee imaging, 3T MRI has the advantage of a higher SNR.[1] Many studies have shown that 3T MRI results in comparable or higher performance in visualizing anatomical structures and detecting cartilage or meniscal lesions compared with 1.5T MRI.[2–6] Nevertheless, 3T scanners have potential drawbacks such as increased chemical shift and susceptibility artifacts,[1] and also, the 3T scanners are usually more expensive than the 1.5T scanners. Also, some patients cannot undergo MR imaging using a 3T scanner due to intra-body devices. Therefore, there is a strong need to improve the images obtained by 1.5T MRI.

The advance of image reconstruction technique on knee MRI had been mainly focused on the accelerated acquisition, and various techniques have been applied. Parallel imaging

[1]Department of Radiology, Institute of Medical Science, University of Tokyo, Tokyo, Japan
[2]Department of Radiology, International University of Health and Welfare Narita Hospital, Narita, Chiba, Japan
[3]Department of Radiology, Graduate School of Medicine, University of Tokyo, Tokyo, Japan
[4]Department of Radiology, International University of Health and Welfare Mita Hospital, Tokyo, Japan
[5]Department of Radiology, International University of Health and Welfare, Ohtawara, Tochigi, Japan
*Corresponding author: Department of Radiology, International University of Health and Welfare Narita Hospital, 852, Hatakeda, Narita, Chiba 286-0124, Japan. Phone: +81 476-35-5600, Fax: +81 476-35-5586, E-mail: kiryu-tky@umin.ac.jp

Received: February 6, 2022 | Accepted: May 22, 2022

was firstly used for this purpose,[7] but the disadvantages included a reduced SNR, aliasing, and reconstruction artifacts.[8] Compressed sensing was also employed to this end,[9] although some disadvantages, including image blurring and long post-processing time, were experienced.

In the last decade, deep learning has become increasingly popular and has been used in many applications, such as image processing, speech recognition, and natural language processing.[10] In the field of diagnostic radiology, deep learning has been successfully applied to image segmentation,[11] lesion detection,[12,13] lesion evaluation,[14,15] and recently to image reconstruction. Deep learning reconstruction (DLR), a new denoising algorithm based on deep learning, is now available from CT and MRI vendors.[16] The algorithm reduces image noise and improves the image quality in head MRI of phantoms and healthy volunteers.[17]

We hypothesized that use of a 1.5T MRI scanner and a DLR (Advanced Intelligent Clear IQ Engine) obtain can produce images of the knee as clear as those obtained by 3T MRI. Therefore, we compared the objective and subjective image qualities of 1.5T/DLR images with 3T images of healthy volunteers. Also, in order to show the image quality improvement by the DLR clearly, image quality of 1.5T image was compared as well.

Materials and Methods

This study was approved by the International University of Health and Welfare Chiba District Ethics Review Committee (20-Nr-059). The written informed consent was obtained from all subjects. All experiments were performed in accordance with the relevant guidelines and regulations. Twenty-one healthy volunteers (17 men and 4 women; mean age ± standard deviation [SD], 44.7 ± 10.9 years) were enrolled in the study (high resolution imaging setting test). Additional six healthy volunteers (6 men; mean age ± SD, 42.2 ± 10.1 years) were assigned to testing with normal resolution image.

MRI examination

All volunteers underwent 3T (Vantage Galan; Canon Medical Systems, Tochigi, Japan) and 1.5T MRI (Vantage Orian; Canon Medical Systems) on the same day using the 16-channel knee coil (16ch Tx/Rx Knee SPEEDER; Canon Medical Systems) and a proton density-weighted image of the right knee was obtained in the coronal plane. The interval between the two scans was less than 15 mins, and similar imaging parameters were used (TR: 2300 ms, TE: 36 ms, number of averages: 1, echo train length: 7 for 1.5T and 8 for 3T, flip angle: 90°, pixel bandwidth: 244 Hz for 1.5T and 488 Hz for 3T, FOV: 150 mm, acquisition matrix: 320 × 256, acceleration factor SPEEDER: 2). To suppress chemical shift artifacts, we apply different bandwidths on 1.5T and 3T, respectively. For the high resolution image, slice thickness was 1 mm, spacing between slices was 1.2 mm, and 40 slices were scanned in a scan time of 2 min 14 sec. For the normal resolution image, slice thickness was 3 mm, spacing between slices was 0.6 mm, and 20 slices were scanned in a scan time of 67 sec.

DLR technique

The DLR technique used in the present study was implemented using a commercially available system, the Advanced Intelligent Clear IQ Engine (AiCE; Canon Medical Systems), as with a former paper.[17] The technique (AiCE) is based on a convolutional neural network (CNN), implemented using the Chainer neural network framework, without skipping of the connections featured in the residual neural networks and composed of one feature extraction (convolutional) layer, 22 feature conversion (convolutional) layers, and one image generation (deconvolutional) layer (Fig. 1). The convolution algorithm using 7×7 discrete cosine transform (DCT) divides the image data into a zero-frequency component and other high-frequency components at the feature extraction layer. The zero-frequency component follows a separate collateral path, and this process allows us to maintain the image contrast regardless of the scan type. Meanwhile, the other 48 high-frequency components are processed as feature maps in the 22 subsequent feature conversion layers. Through this process, DLR can learn parameters to remove noise and restore the lost detailed structure. In each layer, a soft-shrinkage activation function is used to obtain adaptive denoising at various noise levels.[18] Finally, in the image generation layer, deconvolution using a 7×7 inverse DCT kernel is conducted for the feature extraction path data, and the low-pass-filtered image from the zero-frequency component path is added.

The abovementioned CNN was trained using data from 150 knee MRI examinations acquired from healthy volunteers. All images were acquired on a 3T MRI scanner (Vantage Galan 3T ZGO; Canon Medical Systems). The high signal-to-noise ground-truth images of T1-weighted imaging (WI), T2WI, fluid attenuated inversion recovery, T2*WI, and proton density-WI were acquired using 10 averaged repetitions with in-plane rigid registration. Next, pairs of high signal-to-noise ground-truth images and noisy input images, which were obtained by adding Gaussian noise with amplitude between 0% and 20% of the maximum intensity of the ground-truth image, were inputted into the deep learning system to create a model for denoising the MR images. The training data pairs were augmented through horizontal and vertical flip, and also each pair was divided into nine patches to obtain 32400 training image pairs. Since the training was done using the high-frequency components of various contrasts as described above, the MR contrast that DLR can denoise is flexible.

Deep learning was performed using a computer with an NVIDIA Quadro P6000 (Nvidia, Santa Clara, CA, USA) graphics processing unit. Through the training, the threshold coefficient in the soft-shrinkage activation function in all the layers of the CNN and 3×3 convolution kernels in the

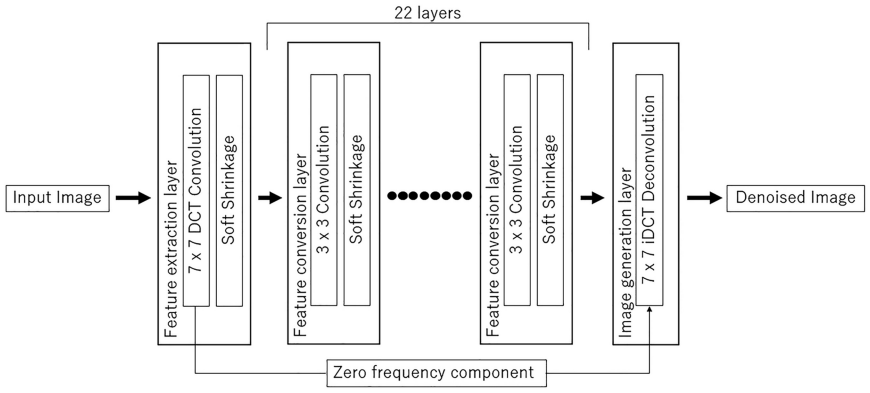

Fig. 1 Schematic of the architecture of the DLR algorithm. DLR, deep learning reconstruction.

Table 1 Scales used for subjective image quality analysis

Grade	Visibility	Noise	Artifact	Overall
1	Not visible	Unacceptable noise	Unacceptable artifact	Unacceptable
2	Mostly not visible or blurred	Strong noise but still diagnostic	Strong artifact but still diagnostic	Average
3	Mostly visible but partially blurred	Acceptable noise	Acceptable artifact	Fair
4	Subtle heterogeneity or blurring	Minimal noise	Minimal artifact	Very good
5	Homogeneous internal intensity with sharp edge	No noise	No artifact	Excellent

feature conversion layers were optimized. These parameters were determined by minimizing a loss function based on mean square error. The Adam iterative stochastic optimization method was used as an optimizer with a learning rate of 0.0001. The CNN has trained 400 epochs with batch size 8, and the total training time was approximately 40 hours.

We used the DLR technique to process the 1.5T MR images and created 1.5T/DLR images.

Subjective evaluation of image quality

Two board-certified radiologists with 12 and 8 years of experience performed subjective assessments of the image quality. They were blinded to the image acquisition method and independently assessed the subjective image quality. The data sets (all 40 coronal images per subject) were analysed in random order to reduce recall bias. Subjective image analysis was assessed in terms of visibility of the structures (anterior cruciate ligament [ACL], medial collateral ligament [MCL], medial meniscus [MM], lateral meniscus [LM], articular cartilage of the medial femoral condyle [MC], articular cartilage of the lateral femoral condyle [LC], and bone), image noise, artifact, and overall diagnostic acceptability. All of these factors were scored on five-point scales, as shown in Table 1.

Objective evaluation of image quality

For objective evaluation of image contrast, we evaluated the signal ratios of the meniscus and the articular cartilage of the femoral condyle at the medial and lateral sides. We set a manual ROI covering the entire area of articular cartilage of the femoral condyle and tibial condyle at the slice which the cartilage showed maximum thickness (Fig. 2a). For the ROI of meniscus, a ROI covering the entire meniscus at the middle body was set (Fig. 2b). The averaged signal intensity of the articular cartilage of the femoral condyle and tibial condyle was recorded as the mean signal intensity of the articular cartilage. Contrast was calculated by dividing the mean signal intensity of the articular cartilage by that of the meniscus.

In order to calculate the degree of image quality improvement by the DLR, we calculated peak SNR (PSNR) using 1.5T MR images as the reference image and 1.5T/DLR images as the test image. We used ImageJ software (National Institutes of Health, Bethesda, MD, USA) for the quantitative image analysis, and the ROIs were placed by a board-certified radiologist with 18 years of experience.

The abovementioned objective image analysis was also conducted for the normal resolution images.

Statistical analysis

All results are expressed as means $\pm$ SD. Since the Kolmogorov-Smirnov test showed the normality of the continuous variable data, among group differences of the image contrast were compared using one-way ANOVA with Bonferroni post hoc testing. For the subjective image quality, among group differences were compared using the Friedman

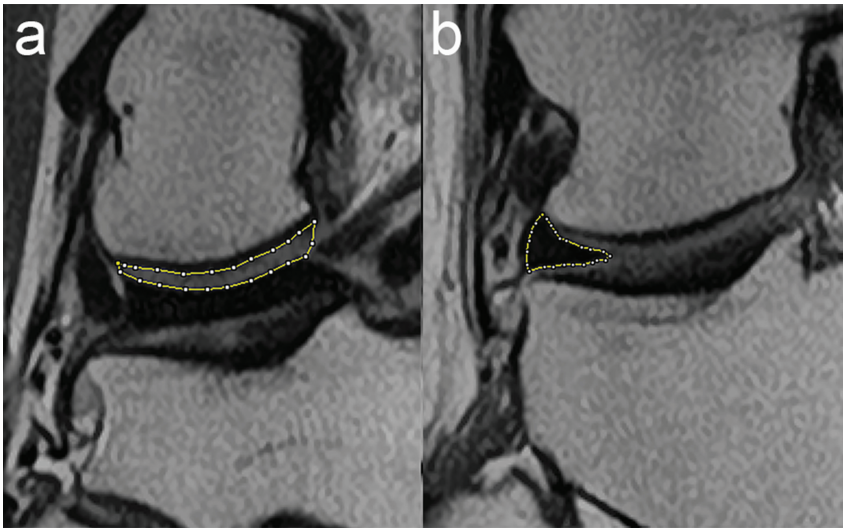

Fig. 2 An example of the ROIs used for subjective analysis of the 1.5T/DLR image quality. (**a**) Articular cartilage of the lateral femoral condyle. (**b**) Middle body of the lateral meniscus. DLR, deep learning reconstruction.

test with Bonferroni post hoc testing. Values of $P < 0.05$ were considered to indicate statistical significance. To evaluate interobserver agreement, we performed Cohen's weighted kappa analysis (quadratic weights), and agreement was categorized according to the Cohen's kappa values as follows: 0–0.20 (poor), 0.21–0.40 (fair), 0.41–0.60 (moderate), 0.61–0.80 (good), and 0.81–1.00 (excellent). Since this analysis will not show the true agreement if the data are highly imbalanced,[19] the concordance rate was recorded in such cases. All statistical analyses were performed using R (version 4.0.5; The R Foundation for Statistical Computing Vienna, Austria).

Results

Deep learning reconstruction was successfully applied to the 1.5T MRI images, and no apparent reconstruction failure image was observed in the 1.5T/DLR images. Representative 1.5T, 1.5T/DLR and 3T images are shown in Figs. 3 and 4.

Subjective analysis of image quality

The results of the subjective analysis are shown in Table 2. Both observers visualized all anatomical structures, except for MC and bone, better on the 1.5T/DLR images than 3T images, with a statistically significant difference (all $P < 0.05$). For the MC, both observers scored better for 1.5T/DLR image, statistical difference was only observed in one observer ($P = 0.002$ and $P = 0.20$). Visualization of bone was similar between the two image types ($P > 0.05$). The level of artifact was also not significantly different. Both observers gave statistically higher scores for image noise (i.e. lower noise) and higher scores for overall diagnostic acceptability on the 1.5T/DLR images compared with the 3T images (both $P < 0.05$). The subjective image scores of 1.5T image were similar to or lower compared to 3T image in all items, and the difference between 1.5T and 1.5T/DLR images was generally more obvious compared to the difference between 1.5T/DLR and 3T images.

Cohen's kappa analysis revealed interobserver agreements of moderate for the visibility of structures (ACL: 0.53, MCL: 0.52, MM: 0.53, LM: 0.50, MC: 0.51, LC: 0.49) and excellent for noise (0.87) and overall image quality (0.81). Additionally, the concordance rate was high for visibility of bone (0.89) and artifact (0.94).

Objective analysis of image quality

The contrast between LM and articular cartilage of lateral condyles was 5.89 ± 1.30 in the 1.5T/DLR image and was higher compared to 1.5T image (3.83 ± 0.68) and 3T image (4.34 ± 0.87) with statistically significant difference (both $P < 0.05$). Also, the contrast between MM and articular cartilage of medial condyles was 5.12 ± 0.93 in the 1.5T/DLR image and was higher compared to 1.5T image (3.46 ± 0.40) and 3T image (3.87 ± 0.56) with statistically significant difference (both $P < 0.05$). PSNR of 1.5T/DLR image compared to 1.5T image was 29.6 ± 1.53 dB, suggesting a successful denoise by the DLR.

Normal resolution image analysis

Representative images are shown in Fig. 5. The contrast between LM and articular cartilage of lateral condyles was 10.8 ± 1.76 in the 1.5T/DLR image and was higher compared to 1.5T image (5.84 ± 0.35) and 3T image (7.37 ± 1.17). Also, the contrast between MM and articular cartilage of medial condyles was 8.34 ± 1.24 in the 1.5T/DLR image and was higher compared to 1.5T image (5.60 ± 0.61) and 3T image (6.82 ± 0.81). PSNR of 1.5T/DLR image compared to 1.5T image was 37.5 ± 0.49 dB, suggesting a higher level of denoise achieved in the high resolution images.

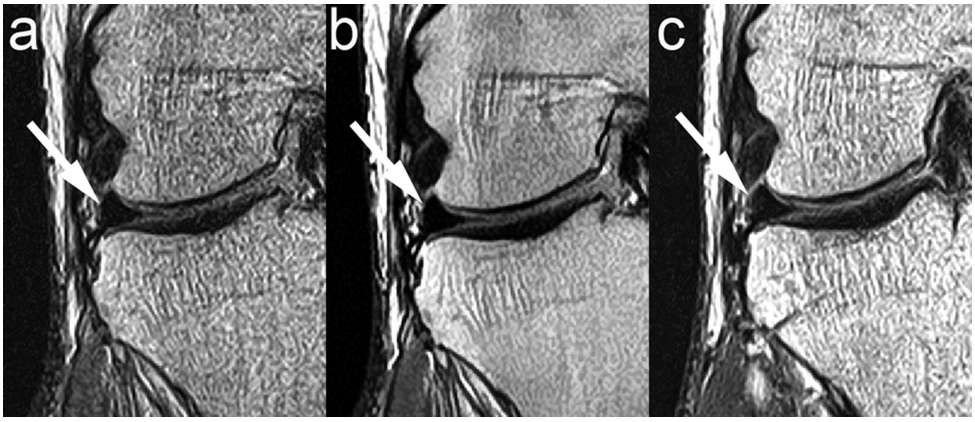

Fig. 3 Representative MR images from a 60 year-old healthy male volunteer. The 1.5T/DLR image (**b**) showed less noise compared with the 1.5T image (**a**) and the 3T image (**c**). Note the clear visualization of the meniscus (white arrow), which scored higher on the 1.5T/DLR image (the two readers assigned a score of 5 for the 1.5T/DLR image and 4 for the both 1.5T and 3T images). DLR, deep learning reconstruction.

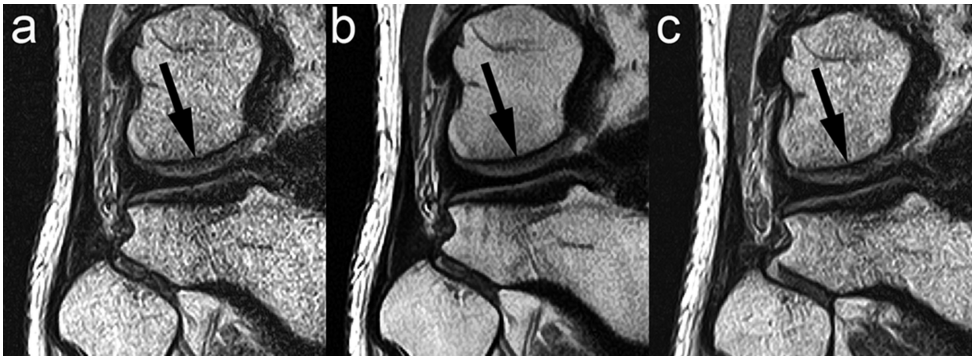

Fig. 4 Representative MR images from a 40 year-old healthy male volunteer. The 1.5T/DLR image (**b**) showed less noise and clearer visualization of articular cartilage (black arrow) compared with the 1.5T image (**a**) and the 3T image (**c**). DLR, deep learning reconstruction.

Discussion

In this study, we showed excellent improvement in image quality by adding DLR to MRI. In the subjective analysis, small (e.g. MM and LM) and large structures (e.g. ACL and MCL) were delineated more clearly on 1.5T/DLR images compared with 3T images, while bone visibility showed no difference. Image noise was significantly lower on 1.5T/DLR images, and the level of artifact was comparable between 1.5T/DLR and 3T images, resulting in higher overall image quality with 1.5T/DLR. The objective image analysis revealed higher SNR and contrast on 1.5T/DLR compared with 3T images.

For the application of DLR in knee MRI, past studies have focused mainly on the technical aspects and more rapid knee MRI scanning.[20] Hammernik et al. successfully reconstructed four-fold accelerated knee MR images using variational network reconstruction.[21] Quan et al. proposed a modified fully residual convolutional auto-encoder and generative adversarial network, which showed superior image quality of the reconstructed image, even for data with an extremely low sampling rate (as low as 10%).[22] Super-resolution is another area of DLR currently being investigated. Chaudhari et al. implemented a 3D CNN called DeepResolve, which was capable of resolving high-resolution thin-sliced knee MR images from lower-resolution thicker-sliced images.[23]

There has been much less research on the clinical application of DLR in knee MRI; only one study has achieved a 5 min comprehensive examination of the knee without compromising image quality or diagnostic accuracy.[24] In that study, Recht et al. performed 406 consecutive knee examinations using a 3T MRI scanner and then evaluated interchangeability. They found a high degree of interchangeability between standard images and deep-learning-based accelerated images.

Our study is unique in that we aimed to improve the quality of 1.5T MRI of the knee using DLR. We showed that 1.5T/DLR images were superior to 3T images both qualitatively and quantitatively. In the quantitative analysis, we assessed the contrast of the articular cartilage and meniscus at the both medial and lateral sides. Both features were improved by 1.5T/DLR imaging, suggesting that articular

Table 2 Results of subjective image quality analysis

	ACL	MCL	MM	LM	MC	LC	Bone	Noise	Artifact	Overall
Reader 1										
1.5T [1/2/3/4/5]	3.33 (0.47) [0/0/14/ 7/0]	4.00 (0.31) [0/0/1/ 19/1]	3.86 (0.47) [0/0/4/ 16/1]	3.95 (0.37) [0/0/2/ 18/1]	2.29 (0.45) [0/15/6/ 0/0]	2.95 (0.21) [0/1/20/ 0/0]	3.95 (0.21) [0/0/1/ 20/0]	2.57 (0.49) [0/9/12/ 0/0]	4.86 (0.64) [0/1/0/ 0/20]	2.52 (0.50) [0/10/11/ 0/0]
1.5T with DLR [1/2/3/4/5]	4.38 (0.79) [0/0/4/ 5/12]	4.76 (0.61) [0/0/2/ 1/18]	4.62 (0.65) [0/0/2/ 4/15]	4.81 (0.50) [0/0/1/ 2/18]	3.29 (0.55) [0/1/13/ 7/0]	3.67 (0.56) [0/1/ 5/15/0]	3.95 (0.21) [0/0/1/ 20/0]	3.95 (0.21) [0/0/1/ 20/0]	4.86 (0.47) [0/0/1/ 1/19]	3.90 (0.29) [0/0/2/ 19/0]
3T [1/2/3/4/5]	3.67 (0.47) [0/0/7/ 14/0]	3.95 (0.58) [0/0/4/ 15/3]	3.95 (0.58) [0/0/4/ 15/3]	4.14 (0.47) [0/0/1/ 16/4]	2.48 (0.50) [0/11/10/ 0/0]	2.95 (0.37) [0/2/ 18/1/0]	3.95 (0.21) [0/0/1/ 20/0]	3.00 (0.00) [0/0/21/ 0/0]	4.95 (0.21) [0/0/0/ 1/20]	3.00 (0.31) [0/1/ 19/1/0]
P-value	0.009	0.001	0.002	0.003	0.002	< 0.001	1.00	< 0.001	1.00	< 0.001
Reader 2										
1.5T [1/2/3/4/5]	3.48 (0.50) [0/0/11/ 10/0]	3.76 (0.43) [0/0/5/ 16/0]	3.19 (0.50) [0/1/15/ 5/0]	3.62 (0.49) [0/0/8/ 13/0]	2.14 (0.35) [0/18/3/ 0/0]	2.67 (0.47) [0/7/14/ 0/0]	4.00 (0.00) [0/0/0/ 21/0]	2.33 (0.47) [0/14/7/ 0/0]	4.95 (0.21) [0/0/0/ 1/20]	2.33 (0.47) [0/14/7/ 0/0]
1.5T with DLR [1/2/3/4/5]	4.24 (0.53) [0/0/1/ 14/6]	4.71 (0.45) [0/0/0/ 6/15]	4.90 (0.29) [0/0/0/ 2/19]	4.86 (0.35) [0/0/0/ 3/18]	3.14 (0.56) [0/2/14/ 5/0]	3.81 (0.39) [0/0/4/ 17/0]	4.10 (0.29) [0/0/0/ 19/2]	4.00 (0.00) [0/0/0/ 21/0]	5.00 (0.00) [0/0/0/ 0/21]	4.00 (0.00) [0/0/0/ 21/0]
3T [1/2/3/4/5]	3.76 (0.43) [0/0/5/ 16/0]	3.95 (0.21) [0/0/1/ 20/0]	3.71 (0.45) [0/0/6/ 15/0]	3.90 (0.29) [0/0/2/ 19/0]	2.86 (0.35) [0/4/16/ 1/0]	3.24 (0.53) [0/1/14/ 6/0]	4.00 (0.00) [0/0/0/ 21/0]	3.00 (0.00) [0/0/21/ 0/0]	4.95 (0.21) [0/0/0/ 1/20]	3.00 (0.00) [0/0/ 21/0/0]
P-value	0.006	< 0.001	< 0.001	< 0.001	0.20	0.015	1.00	< 0.001	1.00	< 0.001

All variables are expressed as mean(standard deviation). Numbers in brackets represent number of cases with each score. *P*-values in the comparison of 1.5T/DLR and 3T images are shown, and items with statistical significant difference are written in bold. ACL, anterior cruciate ligament; DLR, deep learning reconstruction; LC, articular cartilage of the lateral femoral condyle; LM, lateral meniscus; MC, articular cartilage of the medial femoral condyle; MCL, medial collateral ligament; MM, medial meniscus.

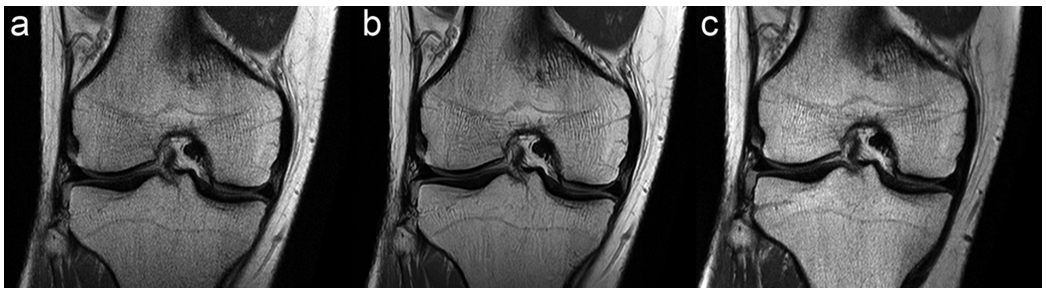

Fig. 5. Representative MR images of normal resolution images. The 1.5T/DLR image (**b**) showed less noise compared with the 1.5T image (**a**) and the 3T image (**c**). DLR, deep learning reconstruction.

cartilage can be evaluated more effectively using 1.5T/DLR than 3T imaging. This is important since a recent meta-analysis study showed greater diagnostic accuracy of 3T MRI over 1.5T MRI, but only for articular cartilage lesions.[6] In this study, although we assessed the efficacy of DLR in knee imaging, 1.5T MR image with DLR may be able to provide images equivalent to or superior to 3T in other musculoskeletal areas, especially those with high susceptibility to artifact induced by air, such as the fingers or toes. Also, although we did not apply the DLR to 3T knee MR images, it is expected to show high quality images since the network is already successfully applied to 3T images in other areas as the brain, cardiac, and female pelvic MRI.[16,17,25]

As described in the result section, we did not encounter reconstruction errors caused by our deep learning technique. The subtracted image before and after applying the reconstruction shows that DLR mainly suppresses noise with Gaussian distribution (See Supplementary Fig. 1 online). Therefore, the DLR may mostly remove the white noise and not delete the internal structures or lesions.

There are several limitations to this study. First, we recruited volunteers at a single institution. As selection bias may have been introduced in our recruitment, our results cannot be generalized. Second, we assessed only proton density-weighted images since it is reported that the image is optimal for detecting meniscal lesions.[26] DLR is reported to be useful in processing various imaging sequences such as T1- and T2-weighted images, fluid-attenuated inversion recovery images, MR cholangiopancreatographic images, and MR coronary angiography.[17,25,27] Thus, we believe that DLR can effectively process other knee MRI sequences as well. Third, although the deep learning reconstruction mainly removes Gaussian noise, 1.5T/DLR image showed different impression on internal structures (especially bone) in some cases. This might be due to the over-fitting of the DLR, although the usefulness of the DLR remains due to their clear visualization of other structures as meniscus and articular cartilage, which are the main targets of knee MRI. Finally, we did not evaluate the detectability of disease. Since DLR significantly improved image quality, we assume that images obtained using DLR would facilitate detection of abnormalities by radiologists, resulting in an improved diagnostic ability. However, further investigations are needed to confirm this assumption.

Conclusion

DLR improved knee MRI significantly, and 1.5T/DLR images were associated with less noise, better visualization of the meniscus and ligaments, and higher overall image quality compared with 3T images obtained using a similar protocol.

Conflicts of Interest

Shigeru Kiryu got research grants from Canon Medical Systems Corporation. Any data and information included in this study was not controlled by Canon Medical Systems Corporation. The other authors have no conflicts of interest to disclose.

Supplementary Information

A supplementary file below is available online.

Supplementary Fig. 1
Subtraction result of the original knee MRI image and post-DLR knee image. The histogram analysis of the subtracted image shows that the image follows a Gaussian distribution.

References

1. Nacey NC, Geeslin MG, Miller GW, Pierce JL. Magnetic resonance imaging of the knee: An overview and update of conventional and state of the art imaging. J Magn Reson Imaging 2017; 45:1257–1275.
2. Wong S, Steinbach L, Zhao J, Stehling C, Ma CB, Link TM. Comparative study of imaging at 3.0 T versus 1.5 T of the knee. Skeletal Radiol 2009; 38:761–769.
3. Grossman JW, De Smet AA, Shinki K. Comparison of the accuracy rates of 3-T and 1.5-T MRI of the knee in the diagnosis of meniscal tear. AJR Am J Roentgenol 2009; 193:509–514.
4. Van Dyck P, Vanhoenacker FM, Lambrecht V, et al. Prospective comparison of 1.5 and 3.0-T MRI for evaluating the knee menisci and ACL. J Bone Joint Surg Am 2013; 95:916–924.
5. Van Dyck P, Kenis C, Vanhoenacker FM, et al. Comparison of 1.5- and 3-T MR imaging for evaluating the articular cartilage of the knee. Knee Surg Sports Traumatol Arthrosc 2014; 22:1376–1384.
6. Cheng Q, Zhao FC. Comparison of 1.5- and 3.0-T magnetic resonance imaging for evaluating lesions of the knee: A systematic review and meta-analysis (PRISMA-compliant article). Medicine (Baltimore) 2018; 97:e12401.
7. Kwok WE, Zhong J, You Z, Seo G, Totterman SM. A four-element phased array coil for high resolution and parallel MR imaging of the knee. Magn Reson Imaging 2003; 21:961–967.
8. Deshmane A, Gulani V, Griswold MA, Seiberlich N. Parallel MR imaging. J Magn Reson Imaging 2012; 36:55–72.
9. Lustig M, Donoho D, Pauly JM. Sparse MRI: The application of compressed sensing for rapid MR imaging. Magn Reson Med 2007; 58:1182–1195.
10. Yasaka K, Akai H, Kunimatsu A, Kiryu S, Abe O. Deep learning with convolutional neural network in radiology. Jpn J Radiol 2018; 36:257–272.
11. Akkus Z, Galimzianova A, Hoogi A, Rubin DL, Erickson BJ. Deep learning for brain MRI segmentation: state of the art and future directions. J Digit Imaging 2017; 30:449–459.
12. Cao L, Shi R, Ge Y, et al. Fully automatic segmentation of type B aortic dissection from CTA images enabled by deep learning. Eur J Radiol 2019; 121:108713.
13. Nakao T, Hanaoka S, Nomura Y, et al. Deep neural network-based computer-assisted detection of cerebral aneurysms in MR angiography. J Magn Reson Imaging 2018; 47:948–953.
14. Yasaka K, Akai H, Kunimatsu A, Abe O, Kiryu S. Deep learning for staging liver fibrosis on CT: a pilot study. Eur Radiol 2018; 28:4578–4585.
15. Kiryu S, Yasaka K, Akai H, et al. Deep learning to differentiate parkinsonian disorders separately using single midsagittal MR imaging: a proof of concept study. Eur Radiol 2019; 29:6891–6899.
16. Ueda T, Ohno Y, Yamamoto K, et al. Compressed sensing and deep learning reconstruction for women's pelvic MRI denoising: Utility for improving image quality and examination time in routine clinical practice. Eur J Radiol 2021; 134:109430.
17. Kidoh M, Shinoda K, Kitajima M, et al. Deep learning based noise reduction for brain MR imaging: Tests on phantoms and healthy volunteers. Magn Reson Med Sci 2020; 19:195–206.
18. Isogawa K, Ida T, Shiodera T, Takeguchi T. Deep shrinkage convolutional neural network for adaptive noise reduction. IEEE Signal Process Lett 2018; 25:224–228.
19. Feinstein AR, Cicchetti DV. High agreement but low kappa: I. The problems of two paradoxes. J Clin Epidemiol 1990; 43:543–549.

20. Johnson PM, Recht MP, Knoll F. Improving the speed of MRI with artificial intelligence. Semin Musculoskelet Radiol 2020; 24:12–20.
21. Hammernik K, Klatzer T, Kobler E, et al. Learning a variational network for reconstruction of accelerated MRI data. Magn Reson Med 2018; 79:3055–3071.
22. Quan TM, Nguyen-Duc T, Jeong WK. Compressed sensing MRI reconstruction using a generative adversarial network with a cyclic loss. IEEE Trans Med Imaging 2018; 37:1488–1497.
23. Chaudhari AS, Fang Z, Kogan F, et al. Super-resolution musculoskeletal MRI using deep learning. Magn Reson Med 2018; 80:2139–2154.
24. Recht MP, Zbontar J, Sodickson DK, et al. Using deep learning to accelerate knee MRI at 3 T: Results of an interchangeability study. AJR Am J Roentgenol 2020; 215:1421–1429.
25. Yokota Y, Takeda C, Kidoh M, et al. Effects of deep learning reconstruction technique in high-resolution non-contrast magnetic resonance coronary angiography at a 3-tesla machine. Can Assoc Radiol J 2021; 72:120–127.
26. Lefevre N, Naouri JF, Herman S, Gerometta A, Klouche S, Bohu Y. A current review of the meniscus imaging: Proposition of a useful tool for its radiologic analysis. Radiol Res Pract 2016; 2016:8329296.
27. Tajima T, Akai H, Sugawara H, et al. Breath-hold 3D magnetic resonance cholangiopancreatography at 1.5T using a deep learning-based noise-reduction approach: Comparison with the conventional respiratory-triggered technique. Eur J Radiol 2021; 144:109994.